

1
2
3
4
5
6
7
8
9
10
11
12
13
14
15
16
17
18
19
20
21
22
23
24
25
26
27
28
29
30
31
32
33
34
35
36
37
38
39
40
41
42
43
44
45
46
47
48
49
50
51
52
53
54
55
56
57
58
59
60
61
62
63
64
65

Cometabolic Biotransformation of 1,4-Dioxane in Mixtures with Hexavalent Chromium Using Attached and Planktonic Bacteria

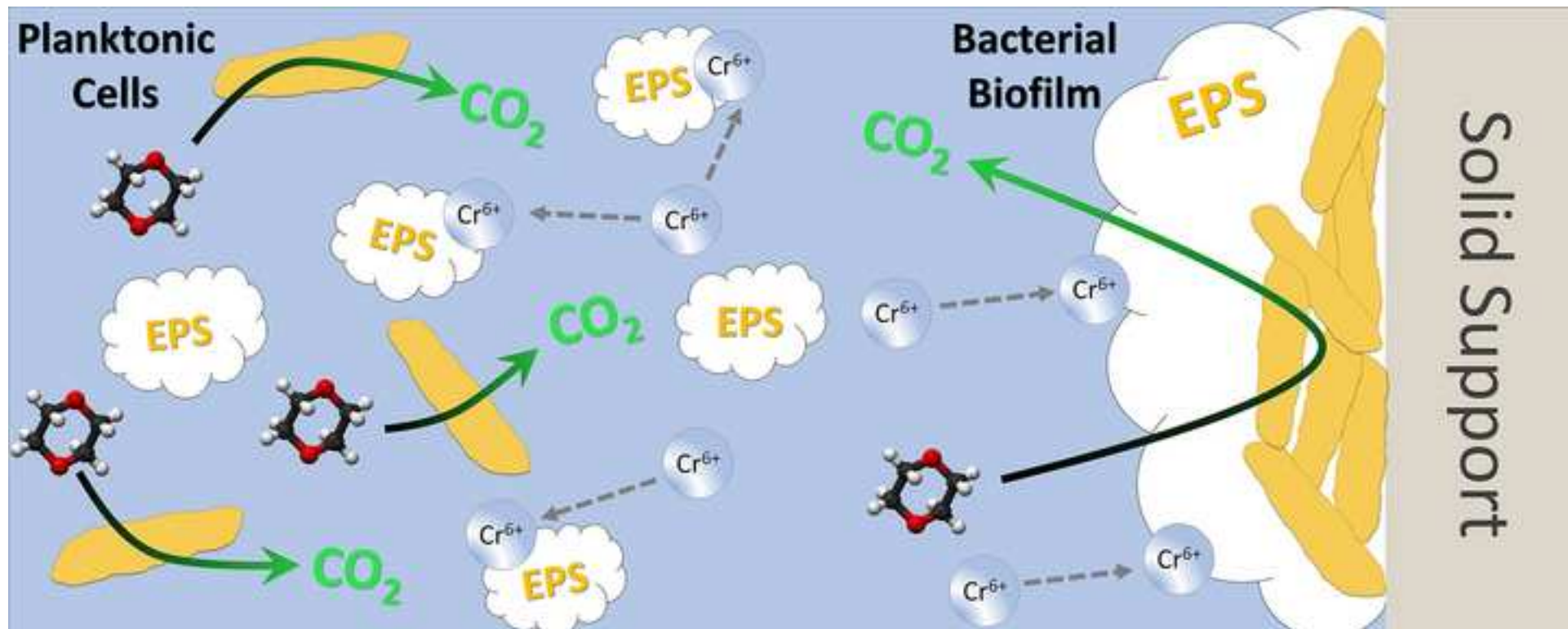
Nicholas W. Johnson¹, Phillip B. Gedalanga^{1,2}, Linduo Zhao³, Baohua Gu³, Shaily Mahendra^{1*}

¹*Department of Civil and Environmental Engineering, University of California, Los Angeles, California, 90095 USA*

²*Department of Public Health, California State University, Fullerton, California 92834, USA*

³*Environmental Sciences Division, Oak Ridge National Laboratory, Oak Ridge, Tennessee, 37831, USA*

**Corresponding author:
email: mahendra@seas.ucla.edu*



- 1,4-Dioxane & Cr(VI) potentially co-occur in groundwater and industrial wastewater
- Planktonic cells and biofilms degraded 1,4-dioxane even in the presence of Cr(VI)
- Biodegradation rates were 10^3 - 10^5 times lower in biofilms than in planktonic cells.
- Exopolysaccharides (EPS) mitigates Cr(VI) inhibition of 1,4-dioxane cometabolism
- 1,4-Dioxane can be successfully biodegraded even in the presence Cr(VI) in water

1 **Abstract**

2 Biological treatment of 1,4-dioxane, a probable human carcinogen and a recalcitrant
3 contaminant of concern, is often complicated by the presence of inhibitory co-
4 contaminants. Due to its use as a solvent, wetting agent, and stabilizer for chlorinated
5 solvents employed in metal vapor degreasing, 1,4-dioxane has often been found to
6 occur with a variety of co-contaminants, including heavy metals such as hexavalent
7 chromium [Cr(VI)]. Cr(VI) also occurs naturally in groundwater due to geological
8 formations, but also has anthropogenic sources that can coincide with 1,4-dioxane from
9 to metal vapor degreasing and and/or discharges from textile dyeing activities.

10 Biodegradation of 1,4-dioxane can be accomplished by microbes that use it as a source
11 of carbon or energy as well as those that cometabolize it after growth on other organic
12 substrates. A propanotroph, *Mycobacterium austroafricanum* JOB5, was grown in
13 planktonic pure cultures and biofilms to determine its ability to cometabolize 1,4-dioxane
14 in the presence of varying concentrations of Cr(VI). 1,4-Dioxane cometabolism by JOB5
15 planktonic cells was uninhibited by Cr(VI) at levels up to 10 mg/L while biofilms were
16 only mildly inhibited at 10 mg/L. As an important part of the biofilms commonly found in
17 subsurface aquifers and engineered systems, extracellular polymeric substances (EPS)
18 were found to play an important role in preventing Cr(VI) exposure to cells. We
19 observed that soluble EPS were able to bind to Cr(VI) and theorize that biofilm-
20 associated EPS additionally served to impede penetration of the biofilm structure by
21 Cr(VI), thus mitigating exposure and toxicity. These findings suggest that bioremediation
22 would be a viable treatment strategy for 1,4-dioxane-contaminated waters that contain
23 elevated levels of Cr(VI) in natural and built environments.

24 **Keywords**

25 Biotransformation, oxyanion, cyclic ether, industrial wastewater, dichromate,
26 exopolysaccharides

27

28 **1.1 Introduction**

29 Recalcitrant contaminants of concern (CoCs), such as the cyclic ether 1,4-
30 dioxane, a probable human carcinogen (IARC, 1999; Zhang et al., 2017), and
31 hexavalent chromium [Cr(VI)], a known human carcinogen (Dayan and Paine, 2001),
32 present challenges when identifying an appropriate strategy due to interactions among
33 compounds and treatment processes. In the context of environmental remediation,
34 many of the source zones or waste streams that involve high concentrations or single
35 contaminants have already been addressed which leaves many sites with large dilute
36 plumes (Adamson et al., 2014). These contamination scenarios at the low end of the
37 concentration scale (in the range of approximately 10-10,000 µg/L) are challenging to
38 both economically and effectively treat (due to reduced kinetics and capital costs that do
39 not necessarily scale to concentration levels) using conventional remedies (DiGuseppi
40 et al., 2016). Beyond groundwater contamination, 1,4-dioxane is also used in the textile
41 industry as a wetting agent for use in various capacities including dye application, and
42 can likely be found in industrial wastewater alongside other contaminants such dyes,
43 other organic compounds, and heavy metals, such as chromium (USEPA, 2006; Zhao
44 et al., 2005). One survey of 27 industrial wastewater treatment plants found 1,4-dioxane
45 and hexavalent chromium concentrations ranging from 0.001-0.315 mg/L and from

46 0.01-0.19 mg/L, respectively (Lee et al., 2015). While the authors did not present data
47 sets for individual wastewater treatment plants that can be used to determine co-
48 occurrence of various compounds, the overall data suggests the possibility of co-
49 occurrence. The complexity found in industrial waste streams and contaminated
50 groundwaters in terms of contaminant mixtures can impose further obstacles to
51 conventional treatments.

52 While several studies have already characterized the inhibition of biological 1,4-
53 dioxane treatment due to chlorinated solvent co-contaminants (Hand et al., 2015;
54 Mahendra et al., 2013; Zhang et al., 2016; Zhao et al., 2018) and some transition metals
55 (Pornwongthong et al., 2014; Zhao et al., 2018), there is limited information on the
56 impact of heavy metals, particularly metallic oxyanions, such as Cr(VI). Chromium is an
57 abundant natural element with speciation that can vary and includes the trivalent [Cr(III)]
58 and hexavalent forms, the most common chemical states of chromium in groundwater
59 (Kimbrough et al., 1999). Cr(III) is generally insoluble in water due to its tendency to
60 form hydroxides, whereas Cr(VI) oxyanions tend to be highly soluble and thus mobile
61 (Cary, 1982). Cr(VI) is a known carcinogen (Dayan and Paine, 2001) and, while no
62 national regulatory standard exists specifically for Cr(VI), USEPA and California do have
63 maximum contaminant levels in place for total chromium of 0.100 and 0.050 mg/L,
64 respectively (SWRCB, 2017). Researchers have demonstrated that hexavalent
65 chromium can negatively impact microbial activity (Novotnik et al., 2014) and have
66 found it in groundwater at concentrations exceeding regulatory standards (Ball and
67 Izbicki, 2004; Hausladen et al., 2018; McPherson et al., 2005). Cr(VI) continues to be an
68 important groundwater contaminant with sources of industrial manufacturing involving

69 metal plating, leather tanning, mining and dressing, pigments (dyes) and refractory
70 alloys (Barnhart, 1997; Kimbrough et al., 1999). A recent study surveyed California
71 Geotracker and found that 7.7% of wells (both supply and monitoring) in California that
72 reported levels greater than 10 µg/L Cr(VI) also contained 1,4-dioxane (Hausladen et
73 al., 2018). The report suggested that the high correlation between 1,4-dioxane and
74 Cr(VI) was likely due to 1,4-dioxane's role as a solvent stabilizer and the historical use
75 of said solvents (particularly 1,1,1-trichloroethane) for vapor degreasing and surface
76 preparation for chrome plating (Hausladen et al., 2018).

77 Previous studies have identified several bacterial strains that can detoxify Cr(VI)-
78 or 1,4-dioxane-contaminated environments using a diverse set of processes. For
79 example, *Mycobacterium* sp. can biosorb over 30 mg/g Cr(VI) (Srinath et al., 2002).
80 Priester et al. (2006) showed that *Pseudomonas putida* can reduce Cr(VI) and bind
81 Cr(III) to extracellular polymeric substances (EPS) in wastewater treatment plants.
82 Similarly, biodegradation of 1,4-dioxane has been established for cometabolic
83 processes by *Mycobacterium austroafricanum* JOB5 (hereafter JOB5) and other
84 monooxygenase-expressing bacteria (Mahendra and Alvarez-Cohen, 2006). Other than
85 Myers et al. (2018), The majority of these studies have focused on the behavior of these
86 microorganisms in planktonic growth modes which may not accurately represent this
87 phenomenon in groundwater or industrial wastewater treatment applications where
88 biofilm growth may be a preferred growth mode. Because bacterial growth modes have
89 distinct physiologies, they may have differential metabolic activity as well as EPS
90 production, which could impact treatment performance, which necessitates not only the
91 consideration of planktonic cells, but biofilms as well.

92 This study focused on exploring the potential of the cometabolic 1,4-dioxane-
93 degrading bacteria JOB5 to biologically transform 1,4-dioxane in the presence of Cr(VI)
94 when grown in biofilms on silica sand and in planktonic suspensions. The results of this
95 study are expected to improve our understanding of contaminant interactions and help
96 determine where biodegradation may be an effective alternative to treat recalcitrant
97 organic pollutants even in mixtures with metal oxyanions in contaminated soils and
98 waters.

99 **1.2 Materials and Methods**

100 **1.2.1 Chemicals**

101 Na₂Cr₂O₇ and 1,4-dioxane (99.8%, ACS grade) were purchased from Sigma-Aldrich (St.
102 Louis, MO). All chemicals in the bacteria culture medium were ACS grade, purity > 99%.
103 Propane (99.9%) was obtained from Matheson Tri-Gas (Basking Ridge, NJ). Silica sand
104 (20-30 mesh, ASTM C-778, Aqua Solutions, Inc.) used for biofilm growth was acid
105 washed using 5% (vol conc. acid/vol DI water) HCl to remove impurities and
106 subsequently washed with deionized water to remove acid residue and acid-mobilized
107 impurities.

108 **1.2.2 Culture Conditions**

109 Propane-oxidizing bacterial cells of JOB5 were grown in pre-sterilized, sealed
110 bottles containing a ratio of 1 part nitrate mineral salts (NMS) medium (Whittenbury et
111 al., 1970) to 4 parts headspace (to ensure sufficient oxygen mass transfer) with 25 %
112 (v/v) filter-sterilized propane added (to ensure stoichiometric excess) into the
113 headspace using sterile syringes. All bottles were incubated at 30°C with 150 rpm

114 agitation. To maintain aerobic conditions, all cell cultures were aerated with filter-
115 sterilized air when the oxygen content fell below 10% as measured using an oxygen
116 and carbon dioxide analyzer (Quantek Instrument, Grafton, MA) followed by adding
117 25% (v/v) propane into the headspace.

118 ***1.2.3 Metabolism of Propane by JOB5 Cells in the Presence of Cr(VI)***

119 The influence of Cr(VI) on propane metabolism by planktonic JOB5 was
120 investigated using batch reactors. JOB5 was prepared in NMS medium as described
121 previously. When the OD₆₀₀ was greater than 1.0, the culture was diluted with NMS
122 medium to achieve an OD₆₀₀ of 0.1 and then placed in a sterile flask with stir bar to
123 ensure it was completely mixed. For all experimental conditions, each 150 mL serum
124 bottle contained 27 mL JOB5 culture and 3 mL Cr₂O₇²⁻ stock solution (or DI water). A
125 range of Cr(VI) concentrations were chosen (0, 0.1, 1, and 10 mg/L) to test the dose-
126 dependent response of JOB5 propane metabolism to hexavalent chromium. The Cr(VI)-
127 free control contained 27 mL JOB5 culture with 3 mL of sterile DI water instead of Cr(VI)
128 stock. Each bottle was closed with a blue butyl rubber stopper and aluminum crimp
129 seal. At the start of the experiment, 6.4 mL of headspace was removed followed by the
130 addition of 6.4 mL propane to achieve 5% (v/v) headspace propane with atmospheric
131 pressure. The bottles were then incubated at 30°C and shaken at 150 rpm. Propane
132 degradation was monitored by measuring propane over the course of the experiment.
133 This experiment was conducted in triplicate.

134 **1.2.4 Cometabolism of 1,4-Dioxane by JOB5 Biofilms in the Presence of**
135 **Cr(VI)**

136 Three chromatographic columns (Kimble Kontes Chromaflex preparatory
137 columns, 2.5 cm I.D. x 30 cm L.) were used as reactors to test the ability of JOB5
138 biofilms to biodegrade 1,4-dioxane in the presence of Cr(VI). A schematic of the column
139 setup is presented as Figure S1 in supporting information (SI). First, a solution of HCl in
140 deionized water (5% vol conc. acid/vol) was recirculated through each column to
141 sterilize the inner surfaces of the experimental apparatuses. The column was then
142 flushed with DI water to remove all acid residue. Autoclave-sterilized sand was then wet
143 packed into each column.

144 To inoculate the sand, JOB5 culture harvested during early exponential phase
145 growth was added (5% v/v) into 500 mL Wheaton serum bottles with 200 mL NMS
146 medium containing 10X KNO₃. The KNO₃ content was elevated to encourage EPS
147 production (Figure S2) as well as increase ionic strength to encourage initial adhesion
148 of JOB5 cells (negative surface charge) with silica sand (negative surface charge) (Hori
149 and Matsumoto, 2010). The bottles were sparged with air to saturate the solution with
150 oxygen followed by the addition of 25% (v/v) headspace propane. One bottle containing
151 JOB5 culture and propane was then connected to each sand-packed column and
152 recirculated in upflow for 14 days at a flow rate of 0.2 mL/min. Oxygen and carbon
153 dioxide levels were monitored as a surrogate for microbial growth and activity. Halfway
154 through the inoculation phase when the oxygen levels in the headspace dropped below
155 10%, 60 mL of filtered ultra-high purity oxygen was added to each serum bottle to bring
156 oxygen levels back up to approximately 21% in the headspace.

157 Following the inoculation phase, 3 pore volumes of sterile, propane-free NMS
158 medium was manually pushed through each column to remove planktonic cells and
159 residual propane using disposable, sterile syringes. At this point the tubing was also
160 changed to the following to remove biofilms not directly associated with the column
161 sand beds. In brief, PTFE (polytetrafluoroethylene) tubing was used for all tubing lines,
162 except for the peristaltic pump tubing (silicone tubing) and the tubing used to make
163 some connections between fittings, to prevent the sorption of 1,4-dioxane. A PTFE filter
164 (0.2 μm membrane, Millipore) was placed directly before the column inlet to prevent
165 contamination of the column biofilms. Polycarbonate 3-way luer-lock valves (Cole-
166 Parmer) were installed directly preceding the influent filter for sample collection. The
167 influent and effluent tubing ends were pushed through rubber stoppers placed over the
168 1 L bottles containing the experimental solutions. Experimental solutions consisted of
169 standard NMS medium containing 1000 $\mu\text{g/L}$ 1,4-dioxane and 0, 1, 10 mg/L Cr(VI).

170 Samples (10 mL) were collected by syringe initially and every 24 hours and
171 analyzed for 1,4-dioxane, Cr(VI), and total chromium. At the conclusion of the
172 experiment, solid samples were collected and evaluated for biomass content by qPCR
173 and EPS content by a protein and polysaccharide assays. Solid sample collection was
174 done by removing sand from both ends of the column using a sterile metal spatula as
175 representative inlet and outlet samples, followed by removing sand until samples could
176 be collected that were representative of the middle of the column bed. Single columns
177 were operated for each condition.

178 **1.2.5 Cometabolism of 1,4-Dioxane by Planktonic JOB5 in the Presence of**
179 **Cr(VI)**

180 The influence of Cr(VI) on 1,4-dioxane cometabolism by JOB5 was investigated
181 at a 1,4-dioxane concentration of 1000 µg/L. JOB5 was prepared in NMS medium as
182 described previously but collected at the end of a feeding cycle (cells in the late
183 exponential phase) and an OD₆₀₀ = 1.0. In all experimental conditions, each serum bottle
184 contained 27 mL JOB5 culture, 3 mL Cr₂O₇²⁻ stock solution, and 300 µL 1,4-dioxane
185 stock solution. A range of Cr(VI) concentrations were chosen (0, 10, 50, 100, 250, and
186 500 mg/L) to test the dose-dependent response of JOB5 1,4-dioxane co-metabolism to
187 hexavalent chromium. The Cr(VI)-free control only contained 30 mL JOB5 culture
188 amended with 1,4-dioxane, while the abiotic control contained 30 mL of NMS medium
189 with 1000 µg/L 1,4-dioxane. Each bottle was closed with a blue butyl rubber stopper and
190 crimp-sealed with an aluminum cap. 1,4-Dioxane samples (200 µL) were collected
191 every 24 hours for the first 3 days and thereafter every 48 hours. 300 µL aqueous
192 samples were collected into 2 mL screw cap tubes and stored at -80°C until ready for
193 total nucleic acids extraction. This experiment was conducted in triplicate.

194 **1.2.6 EPS Extraction**

195 Potential adsorption of Cr(VI) and 1,4-dioxane to soluble EPS (S-EPS), loosely
196 bound EPS (LB-EPS), and tightly bound EPS (TB-EPS; for biofilms only) produced by
197 JOB5 cultures was also investigated. S-EPS were extracted from cell cultures using a
198 modified method described by Tseng et al. (2015). Briefly, 1 mL of planktonic cell
199 culture, 5 mL of column solution, or 1 g of bioaugmented sand in 5 mL of NMS medium
200 was centrifuged at 7000 x g for 10 min and the supernatant, representing the S-EPS

201 fraction, was transferred to a sterile storage tube. An equal volume of NMS medium was
202 then added to the tube containing the pellet and vortex mixed for 5-10 seconds to
203 completely extract LB-EPS. Samples were centrifuged as before and the supernatant
204 was retained for quantification of the LB-EPS fraction. TB-EPS were extracted from
205 biofilm-coated sand using a modified thermal extraction method (Tseng et al., 2015).
206 After completing the previous extraction steps for S- and LB-EPS, an equal volume of
207 NMS (preheated to 50°C) was added to the tube followed by immediate shearing using
208 a vortex mixer for 1 min. The samples were then immediately transferred to a water
209 bath and incubated at 60°C for 30 min. After centrifugation at 7000 x g for 10 min, the
210 resulting supernatant was considered to contain TB-EPS.

211 **1.2.7 Analytical Methods**

212 1,4-Dioxane levels (0-1000 µg/L) in the reactors were quantified using an Agilent
213 6890 gas chromatograph (GC) equipped with a mass spectrometry (MS) detector and a
214 Supelco SPB-1 Sulfur column (30 m x 0.32 mm id x 4 µm) or Restek Rxi-624Sil MS GC
215 column (30 m x 0.25 mm id x 1.4 µm). The collected aqueous sample was processed
216 using a frozen microextraction procedure as described by Li et al. (2010) and the full
217 GC-MS method has been previously described by Zhang et al. (2016). The method
218 detection limit was 5 µg/L.

219 Propane was measured with a Hewlett Packard 6890 gas chromatograph
220 equipped with a flame ionization detector (GC-FID) fitted with a Restek® Stabilwax-DB
221 capillary column (30 m x 0.53 mm x 1 µm). Briefly, 100 µL of headspace was taken
222 directly from the experimental bottles using a gas tight analytical syringe and manually
223 injected into the GC inlet. The injector and detector temperatures were set at 220°C (in

224 splitless mode) and 250°C, respectively. The oven temperature was set to 40°C and
225 held for a method runtime of 2 min. The carrier gas flow (helium) was set to 6.1 mL/min.

226 Total and hexavalent chromium were measured using inductively coupled
227 plasma-optical emission spectrometry (ICP-OES) and EPA Method 7196A, respectively.
228 The details of the analysis are provided in supporting information. The limit of detection
229 was 0.01 and 0.05 mg/L, respectively, for ICP-OES and EPA Method 7196A,
230 respectively.

231 S-, LB-, and TB-EPS protein measurements were performed on the appropriate
232 fraction using the Bradford protein assay, using bovine serum albumin as the standard,
233 by adding 1:1 ratio of sample and Coomassie reagent. Samples were incubated at room
234 temperature for 10 min and absorbance at 595 nm was measured using a Nanodrop
235 spectrophotometer. The polysaccharide fraction of each EPS was quantified by a
236 phenol-sulfuric acid colorimetric method (Dubois et al., 1956) using D-glucose as a
237 standard solution in the range of 2 to 100 mg/L.

238 ***1.2.8 DNA Extraction and Quantification***

239 Total nucleic acids were extracted from samples using a modified phenol-
240 chloroform extraction method as described previously (Gedalanga et al., 2014). Briefly,
241 500 µL of cell cultures were centrifuged at 13,000 x g for 3 min and the supernatant was
242 discarded. After adding 250 µL of lysis buffer (50 mM sodium acetate, 10 mM EDTA [pH
243 5.1]), 100µl 10% sodium dodecyl sulfate, 1.0 ml pH 8.0 buffer-equilibrated phenol, and 1
244 g 100 µm-diameter zirconia-silica beads (Biospec Products, Bartlesville, OK), cells were
245 lysed by heating to 65°C for 2 min, bead beating for 2 min with a Mini-Beadbeater 16

246 (Biospec Products, Bartlesville, OK), incubating at 65°C for 8 min and beads beating
247 again for 2 min. The lysate was collected by centrifugation at 13,000 x g for 5 min
248 followed by phenol/chloroform/isoamyl alcohol purification and chloroform/isoamyl
249 alcohol purification. Precipitation of total nucleic acids was performed by addition of 0.1
250 volume 3 M sodium acetate and 1 volume isopropanol followed by incubation at -20 °C
251 overnight. Nucleic acid pellets were collected by centrifugation at 4°C for 30 min at
252 20,000 g. The precipitate was washed with 70% ethanol and resuspended in 100 µl
253 DNase- and RNase-free water. All samples were stored at -80°C until ready for use.

254 The Universal 16s rRNA gene target (Harms et al., 2003) was quantified by
255 quantitative polymerase chain reaction (qPCR) using an Applied Biosystems StepOne
256 Plus (Life Technologies, Carlsbad, CA). Each reaction consisted of 20 µL containing: 1x
257 Luminaris Color HiGreen/HiROX qPCR Master Mix (Thermo Scientific, Waltham, MA),
258 0.3 mM of primers, and 2 µL of DNA template. The cycling parameters to amplify the
259 gene fragment included 50°C for 2 min, 95°C for 10 min, followed by 40 cycles of 95°C
260 for 15 s and 60°C for 45 s. All reactions were accompanied by a melt curve analysis to
261 confirm the specificity of qPCR products.

262 ***1.2.9 Scanning Electron Microscopy and Energy-Dispersive X-ray Analyses***

263 Energy-dispersive X-ray (EDX) and scanning electron microscopy (SEM)
264 analyses were performed to determine the morphology and elemental composition of
265 planktonic JOB5 cells after exposure to 10 mg/L Cr(VI). After completion of the 1,4-
266 dioxane degradation experiment that included varying levels of Cr(VI), planktonic JOB5
267 cells were prepared following our previously described methods for SEM/EDX analyses
268 (Zhao et al., 2018). Briefly, one droplet of sample suspension was placed on a copper-

269 grid with a carbon film, and then fixed with 2% paraformaldehyde and 2.5%
270 glutaraldehyde. The sample was subsequently washed with sterilized ultrapure water,
271 dehydrated sequentially using increasing proportions of ethanol (from 25% to 100%),
272 and air-dried. The copper-grid was then mounted onto a SEM stub and coated with
273 carbon (to prevent electric charging), and subsequently imaged using a Hitachi S-4800
274 FEG-SEM equipped with energy dispersive X-ray spectroscopy. The SEM was operated
275 at an accelerating voltage of 7-15 kV, and a working distance of 7-10 mm.

276 ***1.2.10 Rate and Rate Constant Calculations***

277 Rate calculations were performed by first using either Microsoft Excel or R
278 software to perform linear regressions on the 1,4-dioxane degradation data. Excel was
279 used when experimental replicates were performed, while R was used when only
280 analytical replicates were available. First order rates were normalized by the biomass
281 measured for each respective reactor. First order rate constants were converted to
282 pseudo-first order rate constants by normalizing each constant by either the average
283 biomass (average of initial and final biomass in the case of batch experiments) or final
284 biomass (in the case of the column experiments). Gene copies measured by qPCR
285 were used as a representative measure of biomass. For ease of comparison, rates and
286 rate constants were also normalized in terms of total protein content by using a
287 correlation between gene copies and protein content (as determined using the Bradford
288 protein assay after solubilizing whole cells using 3 M NaOH and incubating for 30 min).
289 Propagation of error was used to combine standard error calculated for both biomass
290 and concentration data to determine overall standard error values for rates and rate

291 constants (where shown). A detailed description of the calculations performed can be
292 found in SI.

293 **1.3 Results**

294 ***1.3.1 Metabolism of Propane by JOB5 Cells in the Presence of Cr(VI)***

295 The metabolic transformation of propane by active JOB5 culture is presented in
296 Figure 1. The Cr(VI)-free control removed propane similarly to the 0.1 and 1 mg/L Cr(VI)
297 conditions. In the 10 mg/L Cr(VI) condition, JOB5 degraded propane more slowly ($P <$
298 0.5) than each of the other three conditions. In a separate experiment, the effects of
299 higher levels of Cr(VI) on propane consumption by JOB5 were also examined, with
300 results that indicated a clear dose-dependent response (Figure S3).

301 ***1.3.2 Cometabolism of 1,4-Dioxane by JOB5 Biofilms in the Presence of*** 302 ***Cr(VI)***

303 The degradation of 1,4-dioxane observed during the recirculating biofilm column
304 experiments is presented in Figure 2. JOB5 in the 1,4-dioxane-only column
305 cometabolized 1,4-dioxane from an average of 1056 $\mu\text{g/L}$ down to an average of 391
306 $\mu\text{g/L}$ in 9 days. JOB5 in the column with an added 1 mg/L Cr(VI) cometabolized 1,4-
307 dioxane from an average of 1037 $\mu\text{g/L}$ down to an average of 303 $\mu\text{g/L}$ in 9 days. JOB5
308 in the column with an added 10 mg/L Cr(VI) cometabolized 1,4-dioxane from an
309 average of 980 $\mu\text{g/L}$ down to an average of 224 $\mu\text{g/L}$ in 9 days.

310 Samples taken at the end of each experiment were quantified for biomass
311 estimation using qPCR and EPS fraction analyses (Figures 2A and 2C) for bulk solution
312 and at various positions along the column (outlet, middle, inlet). For the qPCR analysis,

313 samples were quantified by universal 16S rRNA amplification. EPS fractions were
314 analyzed by using both polysaccharide and total protein measurements. Both analyses
315 were consistent with each other in terms of relative amounts and distributions of both
316 EPS and gene copies. Fewer than 1% of gene copies found at the various locations on
317 the sand column (ranging from 8.4×10^9 to 4.4×10^{10} copies/g sand across all columns)
318 were detected in bulk solution (ranging from 1.6×10^7 to 2.2×10^8 copies/g solution
319 across all columns). Similar trends were observed for polysaccharide EPS analysis;
320 however, a greater proportion of EPS was found in solution relative to the amount on
321 the sand (approximately 0.01 mg/g solution compared with approximately 0.06 mg/g
322 sand across all columns and EPS fractions). These proportions were approximately
323 constant with no observable trends among EPS fraction, location, and Cr(VI) dose. EPS
324 were also measured for total protein content, but it was found to be below the method
325 detection limit of 1 mg/L for all EPS samples. Cr(VI) and total chromium were also
326 measured to determine if chromium sequestration or reduction may have reduced toxic
327 effects. Cr(VI) levels determined by colorimetric assay remained constant for the
328 duration of the experiment (Figure 2). Total chromium levels measured by ICP-OES
329 were consistent with the Cr(VI) levels measured by EPA Method 7196A, suggesting that
330 no reduction of chromium from the Cr(VI) to Cr(III) redox states occurred during the
331 experiment (Figure 1).

332 Initial transformation rates and rate constants were calculated using the first 5
333 timepoints and normalized to the gene copy numbers averaged over the entirety of each
334 sand column (Table 1). The rates show only a minor effect between 0 and 1 mg/L
335 Cr(VI), with a decrease of the 1,4-dioxane transformation from $4.2 \pm \times 10^{-11}$ to 3.8×10^{-11}

336 $\mu\text{g}/\text{gene copy}\cdot\text{d}$. The rate was approximately halved when the Cr(VI) dose was
337 increased from 1 to 10 mg/L [3.8×10^{-11} to 2.0×10^{-11} $\mu\text{g}/\text{gene copy}\cdot\text{d}$]. Pseudo-first
338 order rate constants were calculated as well. Apparent rate constants were initially
339 calculated for the overall 1,4-dioxane removal trends using linearized forms of pseudo-
340 first order rate laws and ranged from 6.0×10^{-14} to 2.9×10^{-14} L/copy·d for 0-10 mg/L
341 Cr(VI). To account for the experimental setup potentially confounding these overall rate
342 constants, additional calculations were performed using mass balance models for the
343 system to remove any artifacts of the flow rate used on the rate constants. The
344 recirculation reservoir was modeled as an ideal steady flow reactor (Eq. 1).

345
$$V_{\text{reservoir}} \frac{dC_{\text{bulk}}}{dt} = Q \times C_{\text{CE}} - Q \times C_{\text{bulk}} \quad (1)$$

346 Where $V_{\text{reservoir}}$ is the volume of the reservoir, C_{bulk} is the 1,4-dioxane concentration of
347 the solution in the reservoir, t is time, Q is the flow rate, and C_{CE} is the 1,4-dioxane
348 concentration of the column effluent. Because the amount of biomass measured in the
349 reservoirs was $\leq 1\%$ of the total biomass, the 1,4-dioxane biotransformation rates in the
350 reservoirs were assumed to be negligible. The column was modeled as an ideal steady
351 state plug flow reactor (Eq. 2)

352
$$\frac{dC}{d\tau_{\text{column}}} = -kC \quad (2)$$

353 Where C is the 1,4-dioxane concentration of the solution at a distance along the
354 column, τ_{column} is the hydraulic retention time of the column, and k is the first order rate
355 constant for the biodegradation reaction mediated by the biofilm in the column.

356 Integrating and combining the two equations gives the final expression used to extract
357 the rate constant from the degradation time series data (Eq. 3).

$$358 \quad k = \frac{-\ln\left(\frac{V_{reservoir}}{Q} \ln\left(\frac{C_{bulk-t}}{C_{bulk-0}} + 1\right)\right)}{\tau_{column}} \quad (3)$$

359 Where C_{bulk-t} and C_{bulk-0} are the bulk 1,4-dioxane concentrations at time t and time zero.

360 Using this model to extract rate constants from bulk solution measurements yielded

361 larger pseudo-first order rate constant values [1.5×10^{-12} to 6.9×10^{-13} L/copy·d].

362 **1.3.3 Cometabolism of 1,4-Dioxane by Planktonic JOB5 in the Presence of** 363 **Cr(VI)**

364 The degradation results of 1,4-dioxane observed during the batch planktonic
365 experiments is presented in Figure 4. Almost no inhibitory effects were observed for
366 Cr(VI) levels from 0-100 mg/L. Additionally the extents of degradation observed for
367 these conditions were all similar with 1,4-dioxane being biodegraded to below detection
368 within 12 hours. At Cr(VI) levels of 250 and 500 mg/L, drastic reductions in initial
369 biodegradation rates and extents of degradation were observed. After 24 hours, the
370 conditions with 250 and 500 mg/L Cr(VI) reduced average 1,4-dioxane levels from 1166
371 to 690 μ g/L and from 1004 to 902 μ g/L, respectively. No removal was observed in the
372 abiotic control containing only 1,4-dioxane and Cr(VI).

373 Biomass was quantified by qPCR through the amplification of the universal 16S
374 rRNA gene (Figure 3B). No significant changes were found between initial and final
375 gene abundances within each condition. Additionally, gene abundances were similar

376 across all biological conditions. The abiotic control had measurable gene abundances
377 below the level of quantification for the 16S rRNA primers (10^4 copies/mL).

378 Initial transformation rates and rate constants were calculated using the first 5
379 timepoints and normalized to the average gene copy number from initial and final
380 measurements (Table 1). The calculated rates agree well with the observed degradation
381 time series. With Cr(VI) levels from 0-100 mg/L, the 1,4-dioxane degradation rate was
382 approximately 6×10^{-7} $\mu\text{g}/\text{gene copy}\cdot\text{d}$. When Cr(VI) increased to 250 and 500 mg/L,
383 this rate decreased by a factor of approximately 2 and 7.5, respectively [6×10^{-7} to $(3.1$
384 $\pm 0.35) \times 10^{-7}$ and $(8.5 \pm 9.8) \times 10^{-8}$ $\mu\text{g}/\text{gene copy}\cdot\text{d}$, respectively]. Planktonic 1,4-
385 dioxane biodegradation pseudo-first order rate constants were calculated in the same
386 way as the apparent rate constants for the biofilm systems and followed a similar trend
387 as the biofilm rate constants (more inhibition with higher Cr(VI) dose), but inhibition was
388 not observed until Cr(VI) levels reached 250 mg/L, rather than at 10 mg/L for the biofilm
389 systems [(1.5 ± 0.071) - $(1.2 \pm 0.044) \times 10^{-9}$ L/copy·d for 0-100 mg/L Cr(VI); (3.9 ± 0.038)
390 $\times 10^{-10}$ and $(0.24 \pm 4.1) \times 10^{-11}$ L/copy·d for 250 and 500 mg/L Cr(VI), respectively].

391 **1.3.4 SEM-EDX Analysis**

392 SEM-EDX analysis was used to determine the elemental composition of JOB5
393 cell grown in the presence of 10 mg/L Cr(VI) (Figure 5). Figure 5A is an EDX spectrum
394 showing the detection and relative intensities of various elements, including C, O, Cu, S,
395 Al, Si, and K, and Figure 5B shows the SEM photograph of the JOB5 sample that was
396 analyzed. Figure 5C shows overlays of the elemental mapping on the original SEM
397 photograph of the JOB5 cells for 8 elements, including chromium. Relatively large
398 peaks were detected for copper and carbon due to the use of the copper grid and

399 carbon film for holding the sample. Small peaks, such as silicon, potassium, and sulfur,
400 are typical of biological samples. Chromium was below the detection limit, suggesting
401 that it was not accumulated in significant amounts in the cells.

402 **1.4 Discussion**

403 Co-contaminant impacts on the biotransformation of 1,4-dioxane has only
404 recently begun to be considered. Much work has been done to determine the effect of
405 the more obvious chlorinated solvent co-contaminants on 1,4-dioxane biodegradation,
406 but relatively little work has been done that examines the impacts of metals. The
407 published studies that have considered how transition metals may impact
408 biodegradation have focused on metals such as Cu(II), Ni(II), Zn(II), and Cd(II) which
409 are important bacterially micronutrients that can play roles as enzymatic cofactors
410 (Pornwongthong et al., 2014). However, no previous studies have considered the
411 potential impacts of chromium, an important water contaminant and human carcinogen,
412 on the biodegradation of 1,4-dioxane. This is an important gap when the potential co-
413 occurrence of 1,4-dioxane and hexavalent chromium is high considering their common
414 denominator of chlorinated solvents that have historically been extensively used in
415 vapor degreasing processes of metals and metal-plated products (Hausladen et al.,
416 2018) as well as their potential co-occurrence in textile wastewater streams (Lee et al.,
417 2015). Additionally, oxidative in-situ treatments for other contaminants of concern have
418 the potential of mobilizing naturally occurring Cr(III) by oxidizing it to the stable and
419 mobile Cr(VI), thus complicating other pre-existing contaminant plumes (Hausladen et
420 al., 2018).

421 **1.4.1 Observed Inhibition of 1,4-Dioxane Cometabolism by JOB5**

422 This study considered the impact of Cr(VI) on the cometabolic biotransformation
423 of 1,4-dioxane by *Mycobacterium austroafricanum* JOB5, in both planktonic and biofilm
424 growth modes. Cr(VI) did not greatly inhibit 1,4-dioxane cometabolism by JOB5 at levels
425 typical of groundwater (0-1 mg/L) in both planktonic and biofilm systems. Mild inhibition
426 was observed for biofilms when Cr(VI) was increased from 1 to 10 mg/L and inhibition
427 was only observed for planktonic cultures at levels greater than 100 mg/L (specifically
428 250 and 500 mg/L). Beyond these observations, the pseudo-first order rate constants
429 between the planktonic cultures and biofilms were considerably different (by factors of
430 10^3 and 10^5 for apparent or model-extracted rate constants, respectively). This is
431 consistent with previously reported results for the degradation of toluene by
432 *Pseudomonas putida* 54G (with specific activities for planktonic cells being
433 approximately 4 times greater than those for attached cells) (Mirpuri et al., 1997) and for
434 the degradation of chloroform by *Methylosinus trichosporium* OB3b in planktonic
435 cultures (pseudo-first order rate constants of 0.2-0.41 L/mg-VSS) (Speitel et al., 1993)
436 and biofilms (pseudo-first order rate constants of ~0.0001-0.0018 L/mg-VSS) (Speitel
437 and Leonard, 1992). Several factors likely play a role in this apparent rate discrepancy.
438 The specific rates calculated during this study use gene abundance for normalization,
439 which gives a total quantity of a specific gene target rather than the total number of
440 active cells. It is possible that as Mirpuri et al. (1997) found, some of the cells within the
441 biofilm are inactive, thus the gross quantification given by qPCR would overestimate the
442 biomass used to calculate the rate and lead to rate underestimation. This could also be
443 explained by what is understood about biofilms being physiologically distinct from

444 planktonic cells, where gene expression may be considerably different between the two
445 modes which could affect specific degradation rates (Chua et al., 2014). Additionally,
446 the differences in the distribution of EPS possibly played a role with the S-EPS being
447 well dispersed in planktonic reactors, while total EPS were mostly associated with the
448 attached growth cells in the biofilm reactors (rather than dispersed throughout the entire
449 systems). We also examined potential cellular toxicity in terms of primary substrate
450 metabolism, ATP production, and growth (via qPCR) for planktonic cells. Propane
451 metabolism rates were dose-dependent and decreased with increasing Cr(VI) dose
452 (Figures 1 and S3), with noticeable drops in rates with Cr(VI) doses starting at 10 mg/L.
453 Additionally, decreasing trends in both ATP production and 16S rRNA gene copy
454 numbers with increasing Cr(VI) doses (ranging from 0 to 100 mg/L) confirm Cr(VI) toxic
455 effects on JOB5 (Figure S4). However, the exact mechanism of toxicity remains
456 unknown. The inhibitory substrate concentration for Cr(VI) (IC_{50} ; defined as the level of
457 Cr(VI) needed to reduce substrate transformation rates by 50%) was considerably
458 higher for 1,4-dioxane cometabolism than propane metabolism (195.9 vs. 18.08-23.13
459 mg/L, respectively, Table S2).

460 Our results clearly indicate that beyond a threshold, hexavalent chromium does
461 cause inhibitory effects as evidenced by the dose-dependent response of 1,4-dioxane
462 transformation rates observed at even higher levels. However, the effects are not nearly
463 as pronounced as those observed for other transition metals such as Cu(II), Ni(II), and
464 Cd(II). Several different studies have examined the impacts of divalent copper ions on
465 1,4-dioxane transformation in both planktonic and biofilm growth modes
466 (Pornwongthong et al., 2014; Zhao et al., 2018). Pornwongthong et al. (2014) found that

467 the addition of 1 mg/L and 10 mg/L Cu(II) resulted in a 40% and 90% decrease in
468 respective 1,4-dioxane degradation relative to metal-free control rates for the 1,4-
469 dioxane metabolizing strain *Pseudonocardia dioxanivorans* CB1190. Zhao et al. (2018)
470 found that after the addition of 10 mg/L Cu(II) to groundwater containing 10 mg/L 1,4-
471 dioxane used as feedwater for CB1190-bioaugmented soil columns, relative removal
472 decreased from 84% to 58%, an overall decrease in removal efficiency of 31%. While
473 no studies have considered the effects of Ni(II) and Cd(II) on 1,4-dioxane
474 biodegradation by bacterial biofilms, Pornwongthong et al. (2014) found that in addition
475 to Cu(II), Ni(II) and Cd(II) could negatively impact planktonic metabolic 1,4-dioxane
476 biodegradation rates by CB1190 by 35 and 36%, respectively, relative to metal-free
477 rates. No studies have considered the impacts of these transition metals on cometabolic
478 biodegradation of 1,4-dioxane. At environmentally and industrial wastewater relevant
479 concentrations, Cr(VI) does not present much antagonistic potential to 1,4-dioxane
480 cometabolic biotransformation by propanotrophs, such as JOB5.

481 **1.4.2 Inhibition Mitigation by Reduction**

482 While a number of other studies have found that Cr(VI) can negatively impact
483 xenobiotic biodegradation, we found Cr(VI) to have little impact on cometabolic 1,4-
484 dioxane biotransformation by planktonic cells or biofilms. Reduction of Cr(VI) was
485 investigated as a potential mechanism of inhibition mitigation. Studies reported in the
486 literature have demonstrated that Cr(VI) can be both intra- and extracellularly
487 biologically reduced under both oxic and anoxic conditions (Ahemad, 2014). During
488 experiments with Cr(VI), no precipitate was observed, suggesting that no extracellular
489 biologically or abiotically catalyzed reduction was occurring. Because JOB5 is aerobic,

490 the reactors were never placed under anoxic (and potentially reducing) conditions due
491 to the microbial oxygen demand. Additionally, during the biofilm study, the levels of
492 Cr(VI) were found to remain constant during the course of the experiment (Figure 2).
493 When investigated using SEM-EDX, no chromium was found in samples of exposed
494 planktonic JOB5 cells, suggesting that the adsorbed or precipitated Cr was very low, if
495 any (Figure 5). Additionally, tests were conducted with permeabilized planktonic cells to
496 determine if Cr(VI) was being intracellularly reduced to Cr(III), however no decrease in
497 Cr(VI) was observed (Figure S5). Lastly, we measured Cr(VI) and total chromium during
498 the biofilm study to determine if Cr(VI) was being removed or potentially converted to
499 another redox state. No decrease in Cr(VI) or total chromium was observed over the
500 duration of the experiment (Figure 2).

501 **1.4.3 Inhibition Mitigation by EPS**

502 Metal sequestration by biosorption has been demonstrated by a number of
503 studies. Metals have been shown to be sorbed by both cells and EPS (Gupta and
504 Diwan, 2017; Jobby et al., 2018). Experiments with washed, heat killed, and dried
505 planktonic cells demonstrated no Cr(VI) removal by cell membranes (Figure S5). S-EPS
506 produced by planktonic cells were found to be capable of binding Cr(VI) and preventing
507 color development using EPA method 7196A suggesting a level of sorption or chelation
508 ability (Figure S7). These results suggest that S-EPS (for planktonic studies) and total
509 EPS (for biofilm studies), which are comprised primarily of polysaccharides and nucleic
510 acids (Figure S6, Table S1), are responsible for binding Cr(VI) or limiting biofilm cells'
511 exposure, respectively, and thus limiting 1,4-dioxane-biodegradation inhibition due to
512 Cr(VI). This is consistent with work done on EPS derived from activated sludge that

513 found EPS are capable of sorbing Cu, Cd, and Pb (Comte et al., 2008; Guibaud et al.,
514 2009). Chromate has been demonstrated to enter bacterial cells via active transport
515 through sulfate transport systems, specifically sulfate permeases (Aguilar-Barajas et al.,
516 2011; Ahemad, 2014; Cervantes et al., 2001). These transport systems are specific with
517 respect to sulfate and thiosulfate, but are also capable of transporting their structural
518 analogs such as the oxyanions selenate, tungstate, molybdate, and chromate (Aguilar-
519 Barajas et al., 2011). If Cr(VI), in the form of chromate, is bound to EPS, steric
520 hindrances would prevent transmembrane transport, thus preventing uptake by the cells
521 and resulting toxicity. While this prevents cellular uptake and downstream toxic effects,
522 it does not sequester Cr(VI) irreversibly. As previously stated, JOB5-produced S-EPS
523 primarily consist of polysaccharides, a rich carbon and energy source. We considered
524 the possibility of breakdown of S-EPS by resting JOB5 cells without primary substrate,
525 but found no evidence suggesting that JOB5 could use EPS as a growth substrate
526 (Figure S8). Additionally, while no Cr(VI) removal was observed in the biofilm
527 experiment, it is well understood that the EPS that form the matrix of biofilms can
528 impede the penetration of antimicrobial agents from bulk solution to the cells within the
529 biofilm structure, thus mitigating exposure (Davies, 2003).

530 While EPS play a role in mitigating biotransformation inhibition by JOB5, it is
531 possible that other mechanisms could also play a role. Several studies have found that
532 other *Mycobacteria* are capable of resistance to other heavy metals including Cu, Hg,
533 and Zn through metal ion efflux pumps, which is one of the more common forms of
534 metal resistance in addition to reduction strategies (Erardi et al., 1987; Meissner and
535 Falkinham, 1984; Nies, 2003). It is possible that JOB5 carries genes that enable this

536 type of resistance for chromium, however the full genome of this microorganism has not
537 yet been sequenced. Other less common resistance strategies exist, however due to
538 our direct observations of the role that EPS play in binding Cr(VI), these resistance
539 mechanisms were not investigated.

540 **1.4.4 Environmental Applications**

541 Cometabolic biotransformation remains a viable 1,4-dioxane treatment strategy
542 for contaminated water, even with presence of elevated levels of co-contaminants, such
543 as Cr(VI). Overall, we found only minor impacts of Cr(VI) on both extents and rates of
544 1,4-dioxane transformation by *Mycobacterium austroafricanum* JOB5 at environmentally
545 relevant levels [0-10 mg/L Cr(VI) for biofilms and 0-100 mg/L Cr(VI) for planktonic cells].
546 Thus, this treatment method could still be used in both in-situ groundwater remediation
547 and industrial wastewater treatment applications for the biodegradation of 1,4-dioxane,
548 and possibly other organic contaminants of concern. There are several considerations
549 that should be made, however, to exploit cometabolic biodegradation to the fullest,
550 namely the role that EPS play and how they are produced by the bacterium in question.

551 While Cr(VI) has been demonstrated in this study to bind with EPS, this should
552 not be considered a viable Cr(VI) sequestration strategy. Although we found that JOB5
553 was likely not remobilizing Cr(VI) bound to EPS by biodegrading that same EPS, this
554 may not be the case in mixed microbial communities. Because EPS are composed of
555 macromolecules (primarily polysaccharides in the case of JOB5-produced EPS), in a
556 field or engineered application under mixed culture conditions, it is very likely that other
557 microbial community members would be able to utilize EPS as a growth substrate which
558 could remobilize Cr(VI) as a free oxyanion.

559 Additional findings important to the application of JOB5 cometabolism to 1,4-
560 dioxane contamination are the effects of nutrients and oxygen on EPS production. As
561 previously stated, 10x KNO₃ was selected for biofilm experiments because this level of
562 nitrogen encourages more EPS production, which aided (at least in part) biofilm
563 formation on silica sand. The nitrogen to phosphorus (N/P) ratio can have significant
564 ramifications for the levels of EPS produced by microorganisms (Figure S2).
565 Additionally, oxygen deficiency was found to encourage EPS production by JOB5
566 (Figure S9). Elevated EPS levels can have implications for xenobiotic degradation. We
567 found that 1,4-dioxane cometabolism by JOB5 was impeded in a dose-dependent
568 manner by the incremental addition of more EPS (Figure S10). So while EPS appear to
569 play a role in mitigating Cr(VI) toxicity, too much may impede biodegradation of the
570 target organic contaminants of concern, such as 1,4-dioxane.

571 **1.5 Conclusion**

572 1,4-Dioxane cometabolism by *Mycobacterium austroafricanum* JOB5 is resistant
573 to hexavalent chromium inhibition. Most studies focus on planktonic culture behavior
574 when examining biotransformation potential, however in most natural or engineered
575 systems, some combination of planktonic cells and biofilms exists. To this end, we
576 considered how Cr(VI) would impact both planktonic cells and biofilms. Planktonic JOB5
577 cells were completely uninhibited at levels below 100 mg/L Cr(VI), while JOB5 biofilms
578 experienced minor inhibition at 10 mg/L Cr(VI). This suggests that in a system
579 containing both 1,4-dioxane and Cr(VI) at environmentally relevant levels, where
580 bacterial cells were in both growth modes, cometabolic biodegradation would be able to
581 proceed without inhibition. This is surprising considering that Cr(VI) is a known toxicant

582 for many bacteria and is in stark contrast to other metal ions such as Cu(II), Ni(II), and
583 Cd(II) which have demonstrated greater inhibitory effects on 1,4-dioxane biodegradation
584 at similar levels, even though they are essential nutrients as well as catalytic
585 substituents of enzymatic cofactors. While the complete mechanism of resistance
586 remains to be explored, EPS are found to play a role in mitigating Cr(VI) inhibition either
587 by binding with freely dissolved Cr(VI) or by impeding its ability to penetrate biofilms.
588 While this is beneficial in this case, too much EPS can also slow biodegradation
589 kinetics, so it is important to consider factors that may increase EPS production, such
590 as elevated N/P ratios and oxygen limitation. Finally, while Cr(VI) was shown to be
591 sorbed by EPS, this should not be taken as a means of removing Cr(VI) without a
592 mechanism to remove the Cr(VI)-EPS complex from water (that exists for processes
593 such as activated sludge). If employed carefully, cometabolic biodegradation remains
594 an excellent treatment approach for 1,4-dioxane-contaminated waters that contain
595 elevated levels of Cr(VI) in various environments and distribution systems.

596 **Acknowledgements**

597 The authors thank Dr. Shu Zhang, Fiona Guo, and Ly Nguon Tan for assistance with
598 experiments and sample collection, and Maryam Ghavanloughajar and Dr. Sanjay
599 Mohanty for total chromium analyses. We thank Drs. Aaron Jubb and Xiangping Yin at
600 Oak Ridge National Laboratory for technical assistance. This study was supported by
601 Strategic Environmental Research and Development Program [SERDP Contract # ER-
602 2300] and National Science Foundation CAREER Award [# 1255021]. Oak Ridge
603 National Laboratory is managed by UT-Battelle, LLC under Contract No. DE-AC05-
604 00OR22725 with the U.S. Department of Energy.

605

606 **References**

- 607 Adamson DT, Mahendra S, Walker Jr KL, Rauch SR, Sengupta S, Newell CJ. A
608 multisite survey to identify the scale of the 1,4-dioxane problem at contaminated
609 groundwater sites. *Environmental Science & Technology Letters* 2014; 1: 254-
610 258.
- 611 Aguilar-Barajas E, Díaz-Pérez C, Ramírez-Díaz MI, Riveros-Rosas H, Cervantes C.
612 Bacterial transport of sulfate, molybdate, and related oxyanions. *BioMetals* 2011;
613 24: 687-707.
- 614 Ahemad M. Bacterial mechanisms for Cr(VI) resistance and reduction: an overview and
615 recent advances. *Folia Microbiol.* 2014; 59: 321-332.
- 616 Ball JW, Izbicki J. Occurrence of hexavalent chromium in ground water in the western
617 Mojave Desert, California. *Applied Geochemistry* 2004; 19: 1123-1135.
- 618 Barnhart J. Occurrences, uses, and properties of chromium. *Regul. Toxicol. Pharmacol.*
619 1997; 26: S3-S7.
- 620 Cary E. Chromium in air, soil and natural waters. In: Langård S, editor. *Biological and*
621 *environmental aspects of chromium*, 1982, pp. 49-64.
- 622 Cervantes C, Campos-Garcia J, Devars S, Gutierrez-Corona F, Loza-Tavera H, Torres-
623 Guzman JC, et al. Interactions of chromium with microorganisms and plants.
624 *FEMS Microbiology Reviews* 2001; 25: 335-347.
- 625 Chua SL, Liu Y, Yam JKH, Chen Y, Vejborg RM, Tan BGC, et al. Dispersed cells
626 represent a distinct stage in the transition from bacterial biofilm to planktonic
627 lifestyles. *Nature Communications* 2014; 5: 4462.
- 628 Comte S, Guibaud G, Baudu M. Biosorption properties of extracellular polymeric
629 substances (EPS) towards Cd, Cu and Pb for different pH values. *Journal of*
630 *hazardous materials* 2008; 151: 185-193.
- 631 Davies D. Understanding biofilm resistance to antibacterial agents. *Nature reviews Drug*
632 *discovery* 2003; 2: 114.
- 633 Dayan A, Paine A. Mechanisms of chromium toxicity, carcinogenicity and allergenicity:
634 review of the literature from 1985 to 2000. *Hum. Exp. Toxicol.* 2001; 20: 439-451.

- 635 DiGiuseppi W, Walecka-Hutchison C, Hatton J. 1,4-Dioxane treatment technologies.
636 Remediation Journal 2016; 27: 71-92.
- 637 Dubois M, Gilles KA, Hamilton JK, Rebers P, Smith F. Colorimetric method for
638 determination of sugars and related substances. Anal. Chem. 1956; 28: 350-356.
- 639 Erardi F, Failla M, Falkinham J. Plasmid-encoded copper resistance and precipitation by
640 Mycobacterium scrofulaceum. Appl. Environ. Microbiol. 1987; 53: 1951-1954.
- 641 Gedalanga PB, Pornwongthong P, Mora R, Chiang SYD, Baldwin B, Ogles D, et al.
642 Identification of Biomarker Genes To Predict Biodegradation of 1,4-Dioxane.
643 Applied and Environmental Microbiology 2014; 80: 3209-3218.
- 644 Guibaud G, van Hullebusch E, Bordas F, d'Abzac P, Joussein E. Sorption of Cd(II) and
645 Pb(II) by exopolymeric substances (EPS) extracted from activated sludges and
646 pure bacterial strains: modeling of the metal/ligand ratio effect and role of the
647 mineral fraction. Bioresource Technology 2009; 100: 2959-2968.
- 648 Gupta P, Diwan B. Bacterial exopolysaccharide mediated heavy metal removal: a
649 review on biosynthesis, mechanism and remediation strategies. Biotechnology
650 Reports 2017; 13: 58-71.
- 651 Hand S, Wang B, Chu KH. Biodegradation of 1,4-dioxane: Effects of enzyme inducers
652 and trichloroethylene. Science of the Total Environment 2015; 520: 154-9.
- 653 Harms G, Layton AC, Dionisi HM, Gregory IR, Garrett VM, Hawkins SA, et al. Real-time
654 PCR quantification of nitrifying bacteria in a municipal wastewater treatment
655 plant. Environmental science & technology 2003; 37: 343-351.
- 656 Hausladen DM, Alexander-Ozinskas A, McClain C, Fendorf S. Hexavalent Chromium
657 Sources and Distribution in California Groundwater. Environmental science &
658 technology 2018; 52: 8242-8251.
- 659 Hori K, Matsumoto S. Bacterial adhesion: from mechanism to control. Biochemical
660 Engineering Journal 2010; 48: 424-434.
- 661 IARC. Re-evaluation of some organic chemicals, hydrazine and hydrogen peroxide. 71.
662 IARC, Lyon, France, 1999.
- 663 Jobby R, Jha P, Yadav AK, Desai N. Biosorption and biotransformation of hexavalent
664 chromium [Cr (VI)]: a comprehensive review. Chemosphere 2018; 207: 255-266.

- 665 Kimbrough DE, Cohen Y, Winer AM, Creelman L, Mabuni C. Crit. Rev. Environ. Sci.
666 Technol. Critical Reviews in Environmental Science and Technology 1999; 29: 1-
667 46.
- 668 Lee W, Park S-H, Kim J, Jung J-Y. Occurrence and removal of hazardous chemicals
669 and toxic metals in 27 industrial wastewater treatment plants in Korea.
670 Desalination and Water Treatment 2015; 54: 1141-1149.
- 671 Li MY, Fiorenza S, Chatham JR, Mahendra S, Alvarez PJJ. 1,4-Dioxane biodegradation
672 at low temperatures in Arctic groundwater samples. Water Research 2010; 44:
673 2894-2900.
- 674 Mahendra S, Alvarez-Cohen L. Kinetics of 1,4-dioxane biodegradation by
675 monooxygenase-expressing bacteria. Environmental Science & Technology
676 2006; 40: 5435-5442.
- 677 Mahendra S, Grostern A, Alvarez-Cohen L. The impact of chlorinated solvent co-
678 contaminants on the biodegradation kinetics of 1,4-dioxane. Chemosphere 2013;
679 91: 88-92.
- 680 McPherson TN, Burian SJ, Stenstrom MK, Turin H, Brown MJ, Suffet I. Trace metal
681 pollutant load in urban runoff from a Southern California watershed. J. Environ.
682 Eng. 2005; 131: 1073-1080.
- 683 Meissner P, Falkinham J. Plasmid-encoded mercuric reductase in *Mycobacterium*
684 *scrofulaceum*. Journal of bacteriology 1984; 157: 669-672.
- 685 Mirpuri R, Jones W, Bryers JD. Toluene degradation kinetics for planktonic and
686 biofilm-grown cells of *Pseudomonas putida* 54G. Biotechnology and
687 bioengineering 1997; 53: 535-546.
- 688 Myers MA, Johnson NW, Zerecero Marin E, Pornwongthong P, Liu Y, Gedalanga PB, et
689 al. Abiotic and bioaugmented granular activated carbon for the treatment of 1,4-
690 dioxane-contaminated water. Environmental Pollution 2018; 240: 916-924.
- 691 Nies DH. Efflux-mediated heavy metal resistance in prokaryotes. FEMS microbiology
692 reviews 2003; 27: 313-339.
- 693 Novotnik B, Zuliani T, Ščančar J, Milačič R. Inhibition of the nitrification process in
694 activated sludge by trivalent and hexavalent chromium, and partitioning of
695 hexavalent chromium between sludge compartments. Chemosphere 2014; 105:
696 87-94.

- 697 Pornwongthong P, Mulchandani A, Gedalanga PB, Mahendra S. Transition metals and
698 organic ligands influence biodegradation of 1,4-dioxane. Applied Biochemistry
699 and Biotechnology 2014; 173: 291-306.
- 700 Priester JH, Olson SG, Webb SM, Neu MP, Hersman LE, Holden PA. Enhanced
701 exopolymer production and chromium stabilization in *Pseudomonas putida*
702 unsaturated biofilms. Applied and Environmental Microbiology 2006; 72: 1988-
703 1996.
- 704 Speitel GE, Leonard JM. A sequencing biofilm reactor for the treatment of chlorinated
705 solvents using methanotrophs. Water environment research 1992; 64: 712-719.
- 706 Speitel GE, Thompson RC, Weissman D. Biodegradation kinetics of *Methylosinus*
707 *trichosporium* OB3b at low concentrations of chloroform in the presence and
708 absence of enzyme competition by methane. Water Research 1993; 27: 15-24.
- 709 Srinath T, Verma T, Ramteke PW, Garg SK. Chromium (VI) biosorption and
710 bioaccumulation by chromate resistant bacteria. Chemosphere 2002; 48: 427-
711 435.
- 712 SWRCB. State water board approves removal of drinking water standard for hexavalent
713 chromium. SWRCB, Sacramento, CA, 2017.
- 714 Tseng LY, Gori R, Rosso D. Effects of activated sludge process conditions on the
715 production of extracellular polymeric substances: Results of yearlong monitoring
716 in a warm climate. Environmental Engineering Science 2015; 32: 582-592.
- 717 USEPA. Treatment technologies for 1,4-dioxane: Fundamentals and field applications.
718 USEPA, 2006.
- 719 Whittenbury R, Phillips KC, Wilkinson JF. Enrichment, isolation and some properties of
720 methane-utilizing bacteria. J Gen Microbiol 1970; 61: 205-18.
- 721 Zhang S, Gedalanga PB, Mahendra S. Biodegradation kinetics of 1,4-dioxane in
722 chlorinated solvent mixtures. Environmental Science & Technology 2016; 50:
723 9599-9607.
- 724 Zhang S, Gedalanga PB, Mahendra S. Advances in bioremediation of 1,4-dioxane-
725 contaminated waters. Journal of Environmental Management 2017; 204: 756-
726 774.

- 727 Zhao G, Li M, Hu Z, Hu H. Dissociation and removal of complex chromium ions
728 containing in dye wastewaters. *Separation and purification Technology* 2005; 43:
729 227-232.
- 730 Zhao L, Lu X, Polasko A, Johnson NW, Miao Y, Yang Z, et al. Co-contaminant effects
731 on 1,4-dioxane biodegradation in packed soil column flow-through systems.
732 *Environmental Pollution* 2018; 243: 573-581.
- 733

Table 1. Initial 1,4-Dioxane^a Cometabolic Degradation Rates

Growth Mode	Initial Cr(VI)	Rate ± SE ^b		Apparent ^c Rate Constant ± SE ^b		Modeled ^d Rate Constant ± SE ^e	
	mg/L	µg _{1,4-dioxane} /copy-d	µg _{1,4-dioxane} /mg protein·d ^f	L/copy-d	L/mg protein·d ^f	L/copy-d	L/mg protein·d ^f
Biofilm	0	4.2 x 10 ⁻¹¹	1.4	6.0 x 10 ⁻¹⁴	2.1 x 10 ⁻³	1.5 ± x 10 ⁻¹²	5.2 x 10 ⁻²
Biofilm	1	3.8 ± x 10 ⁻¹¹	1.3	5.7 x 10 ⁻¹⁴	2.0 ± x 10 ⁻³	1.2 x 10 ⁻¹²	4.1 x 10 ⁻²
Biofilm	10	2.0 ± x 10 ⁻¹¹	0.68	2.9 ± x 10 ⁻¹⁴	1.0 ± x 10 ⁻³	6.9 x 10 ⁻¹³	2.4 x 10 ⁻²
Planktonic	0	(5.5 ± 0.065) x 10 ⁻⁷	(1.7 ± 0.021) x 10 ⁴	(1.5 ± 0.071) x 10 ⁻⁹	(4.4 ± 0.21) x 10 ²	-	-
Planktonic	10	(6.3 ± 0.29) x 10 ⁻⁷	(1.9 ± 0.089) x 10 ⁴	(1.5 ± 0.061) x 10 ⁻⁹	(3.6 ± 0.15) x 10 ²	-	-
Planktonic	100	(6.4 ± 0.23) x 10 ⁻⁷	(2.0 ± 0.072) x 10 ⁴	(1.2 ± 0.044) x 10 ⁻⁹	(4.0 ± 0.14) x 10 ²	-	-
Planktonic	250	(3.1 ± 0.35) x 10 ⁻⁷	(9.5 ± 1.1) x 10 ³	(3.9 ± 0.038) x 10 ⁻¹⁰	(1.3 ± 0.13) x 10 ²	-	-
Planktonic	500	0 ^g	0 ^g	0 [*]	0 [*]	-	-

^aInitial 1,4-dioxane levels were 1000 µg/L in all experiments.

^bSE = Standard Error; Standard errors were not included for biofilm experiments because they would only reflect analytical error.

^cApparent rate constants determined directly using degradation data and linearized pseudo first order rate model

^dModeled rate constants determined using degradation data and reactor modeling. Rate constants were calculated using the first 5 time points. These 4 rate constants were then averaged.

^eStandard error calculated for the 4 calculated rate constants.

^fTotal protein content was determined using the Bradford protein assay.

^{g,h}Rates and rate constants were not statistically different from 0 (P=0.95 and P=0.43 , respectively) using a two-tailed t-test.

Figure 1

[Click here to download Figure: STOTEN-D-19-09821_Figure1_Final.doc](#)

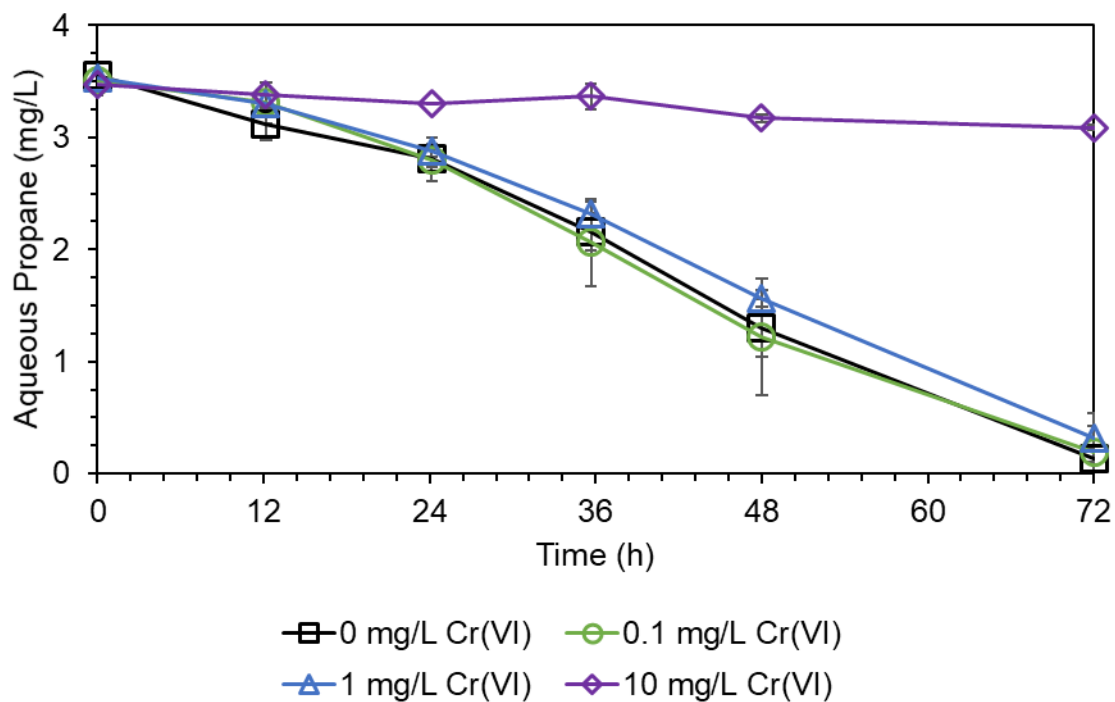


Figure 1. Biodegradation of propane by JOB5 was unaffected by low levels of Cr(VI). JOB5 planktonic batch reactors containing 0, 0.1, and 1 mg/L Cr(VI) were equally able to degrade propane, while 10 mg/L Cr(VI) inhibited JOB5 propane metabolism. Error bars represent the standard deviation of triplicate reactors.

Figure 2

[Click here to download Figure: STOTEN-D-19-09821_Figure2_Final.doc](#)

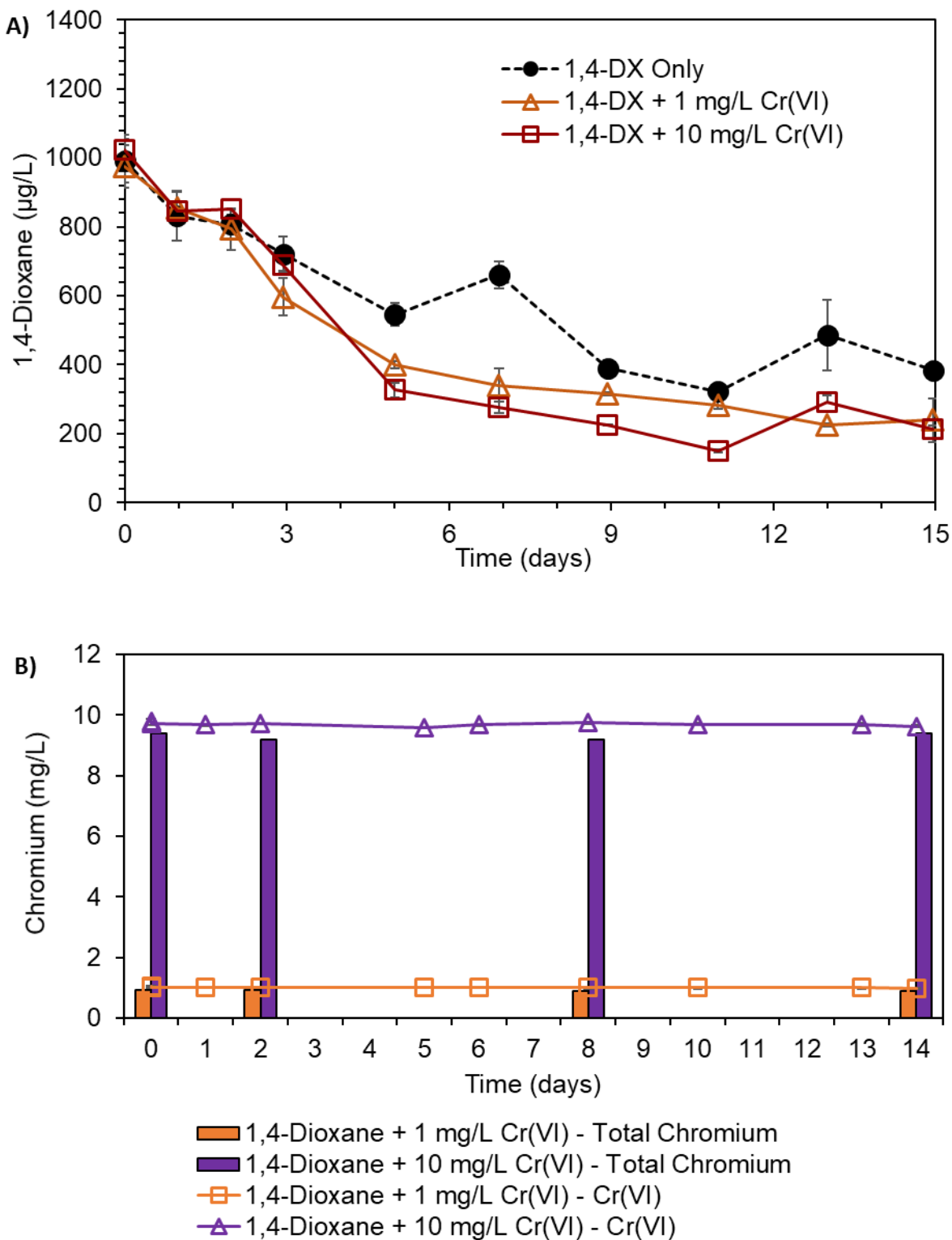


Figure 2. Biodegradation of 1,4-Dioxane in JOB5-Bioaugmented Sand

Columns with no Cr(VI) removal. A) JOB5 biofilms grown on acid-washed silica

sand resisted inhibition by Cr(VI) and biodegraded 1,4-dioxane. Single column experiments were conducted for each experimental condition. Error bars represent half the range of duplicate analytical measurements. B) No significant reduction in Cr(VI) was seen in either the low or high Cr(VI) conditions as evidenced by the minimal differences between Cr(VI) and total chromium measurements for all conditions. Cr(VI) likely appears slightly higher than total chromium due to slight differences in accuracy between the two measurement methods used. Error bars represent the standard deviation of triplicate analytical measurements for hexavalent chromium.

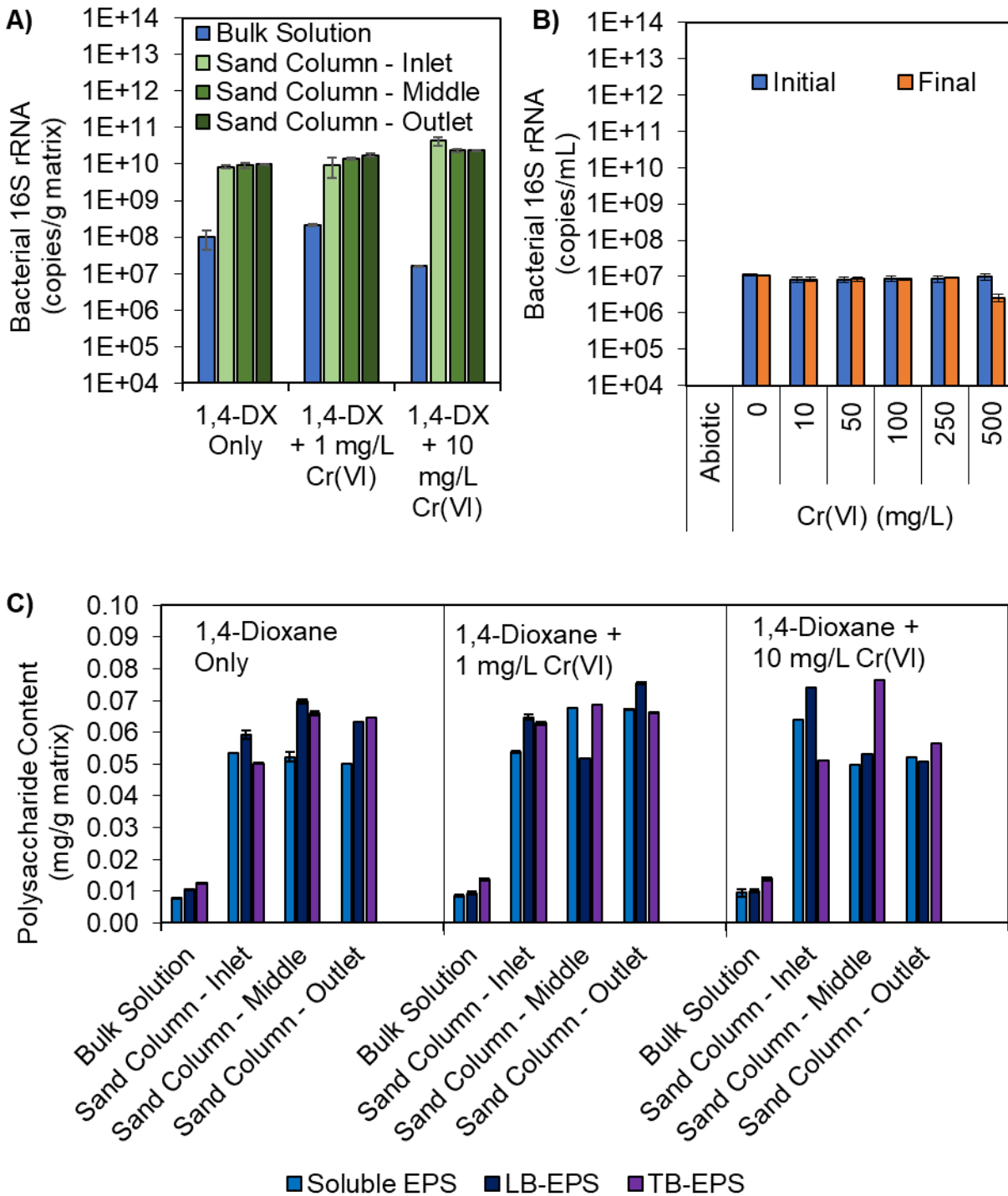


Figure 3. Biomass Quantification by qPCR and EPS Analyses. A) Biofilm biomass results from qPCR analysis using the universal 16S rRNA gene target for biofilm reactors. Error bars represent the standard deviation of triplicate qPCR

reactions. B) Planktonic biomass results from qPCR analysis using the universal bacterial 16S rRNA gene target for planktonic reactors. Error bars represent the standard deviation of triplicate experimental reactors. C) Three EPS fractions (soluble, LB-EPS, and TB-EPS) were extracted from bulk liquid and sand (at three locations within each column: top, middle, and bottom) from the biofilm experiment. EPS was analyzed for both total polysaccharide and protein contents. Total protein content was found to be less than the lower limit of detection (< 1 mg/L) for all samples. Error bars represent the standard deviation of triplicate analytical measurements.

Figure 4

[Click here to download Figure: STOTEN-D-19-09821_Figure4_Final.doc](#)

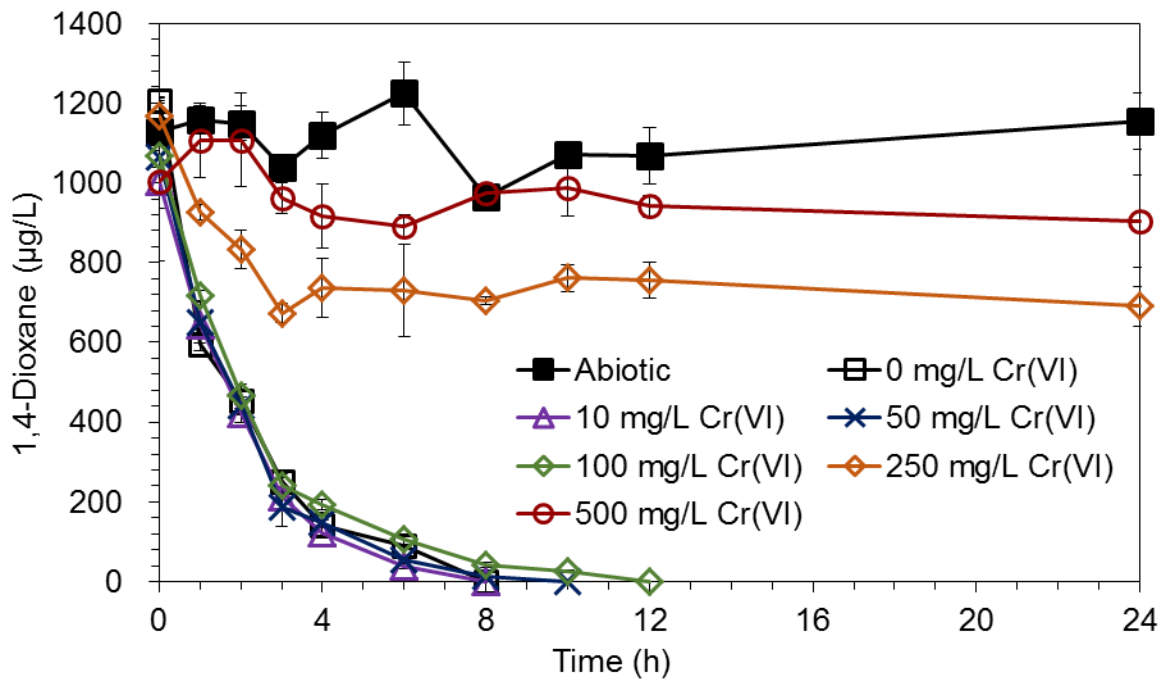


Figure 4. Planktonic JOB5 1,4-Dioxane Cometabolism is Uninhibited by Cr(VI) at Levels as High as 100 mg/L. Error bars represent the standard deviation of triplicate reactors.

Figure 5

[Click here to download Figure: STOTEN-D-19-09821_Figure5_Final.doc](#)

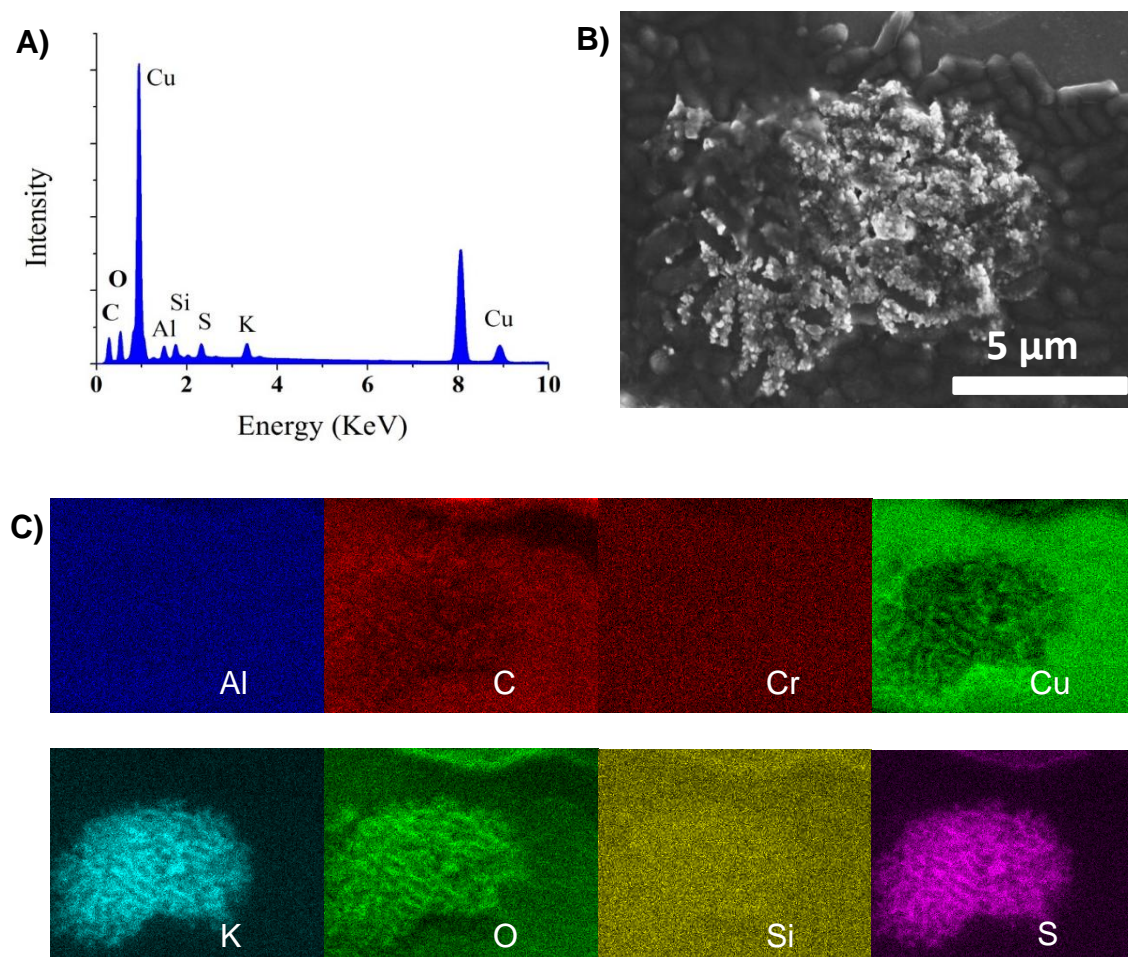


Figure 5. JOB5 Cells Analyzed Using SEM-EDX Spectroscopy. A) Energy dispersive X-ray (EDX) spectroscopy of the JOB5 sample. B) Scanning electron microscopic (SEM) image of the JOB5 cell sample without filtering. C) EDX analyses of elemental composition of the JOB5 sample. No chromium was detected in the sample, due to its low concentrations. Copper signal came from copper grids used for holding the sample.